

Electrostatic Interactions across a β -Sheet[†]Cheryl A. Blasie[†] and Jeremy M. Berg^{*,‡,§}

Department of Chemistry, The Johns Hopkins University, 34th and Charles Street, Baltimore, Maryland 21218, and Department of Biophysics and Biophysical Chemistry, The Johns Hopkins University School of Medicine, 725 North Wolfe Street, Baltimore, Maryland 21205

Received November 13, 1996; Revised Manuscript Received March 7, 1997[®]

ABSTRACT: The free energy consequences of electrostatic interactions across a model β -sheet have been probed using a consensus zinc finger peptide. Relative folding free energies have been deduced from coupled peptide folding/metal binding reactions. The energies of the electrostatic interactions have been isolated via double mutant cycles performed at a series of NaCl concentrations. The observed favorable free energies associated with potential ion pairs are modest, less than 0.5 kcal/mol. Unfavorable interactions due to like-charge pairs of similar magnitude were also observed. The largest effects, both favorable and unfavorable, involved interactions with aspartic acid. These observations are consistent with electrostatic interactions occurring without contact ion pair formation with the larger interaction energies involving aspartic acid being due to the relative lack of flexibility of its side chain.

Ionic interactions such as salt bridges have been structurally observed in a wide range of protein structures. Because of the relatively strong nature of the Coulomb force, such interactions might be expected to have profound effects on protein stability. However, the net energetic effect of such interactions involves a number of other terms in addition to the electrostatic interactions present in the native structure. These include the energetics of the interactions between the charged amino acids and solvent and between these amino acids and other parts of the protein and the loss of side chain conformational entropy associated with the introduction of structure-dependent interactions. The energetics of ionic interactions, particularly salt bridges, have been probed experimentally and theoretically in a number of protein and peptide model systems (Huyghues-Despointes *et al.*, 1993; Horovitz *et al.*, 1990; Lumb & Kim, 1995; Lyu *et al.*, 1992; Marqusee & Baldwin, 1987, 1990; Merutka & Stellwagen, 1991; Sun *et al.*, 1991a; Venugopal *et al.*, 1994). These studies have yielded a number of differing results ranging from substantial stabilization to mild destabilization. Although a number of studies have involved α -helices, there has been no systematic study specifically probing the energetics of electrostatic interactions in a model β -sheet environment.

We present here an investigation of the electrostatic interactions across a β -sheet in the context of a zinc finger peptide, namely, the consensus zinc finger peptide CP-1 (Krizek *et al.*, 1991). The metal-bound, folded form of this peptide is prototypical of this class of domain consisting of an antiparallel β hairpin followed by a helix as shown by

NMR (Vinson *et al.*, 1996) and X-ray crystallography (Kim & Berg, 1996) in Figure 1b. Folding of this zinc finger peptide appears to be a two-state process. In the absence of metal, the peptide appears to be largely or completely unfolded. Upon binding of zinc(II) or cobalt(II), the zinc finger peptide adopts its well-defined tertiary structure (Frankel *et al.*, 1987; Párraga *et al.*, 1988). With the assumption that amino acid sequence changes not involving the metal binding residues do not affect the energetics of the direct interactions between the peptide and the metal ion, changes in experimentally determined metal binding energies can be used as a measure of relative protein folding energies (Krizek *et al.*, 1993) as summarized in Figure 2. We have designed a series of peptides with changes in the residues in positions 3 and 10 across from one another in the β -sheet of CP-1 to probe the energetics of electrostatic interactions in this context. The mutations made to introduce potential salt bridges were K3E10, K3D10, R3D10, and R3E10. The like-charged pairs K3K10, R3R10, D3D10, and E3E10 were also investigated. The “wild-type” sequence has K in position 3 and S in position 10. In many, but not all, cases, the energetics of the electrostatic interactions were evaluated through the use of double mutant cycles (Horovitz *et al.*, 1990).

MATERIALS AND METHODS

All peptides were synthesized using a Milligen/Bioscience 9050 peptide synthesizer and purified as previously described (Krizek *et al.*, 1993). Peptide identities were confirmed by mass spectrometry and were within 1 mass unit of the expected molecular masses. All peptide manipulations were performed in an anaerobic atmosphere containing 5–6% hydrogen in nitrogen to prevent cysteine oxidation.

To determine the metal binding free energies precisely, a competitive two-peptide metal binding assay was developed (Krizek *et al.*, 1993). These metal cotitrations were performed in 100 mM HEPES,¹ pH 7.0, with varying concentrations of sodium chloride. Approximately equimolar amounts of the CP-1(CCHH) variant and CP-1(CCHC)

[†] Supported by NIH Grant GM51362-01.

* Address correspondence to this author at the Department of Biophysics and Biophysical Chemistry, The Johns Hopkins University School of Medicine.

[‡] Department of Chemistry, The Johns Hopkins University.

[§] Department of Biophysics and Biophysical Chemistry, The Johns Hopkins University School of Medicine.

[®] Abstract published in *Advance ACS Abstracts*, May 1, 1997.

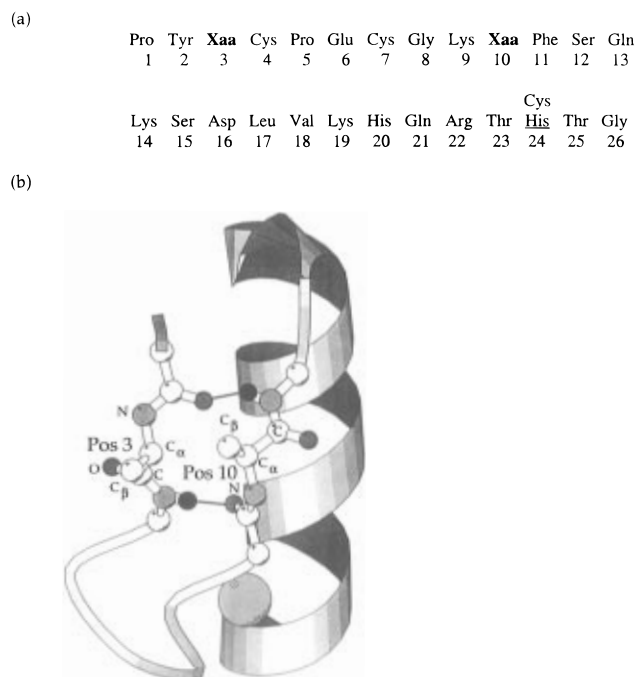


FIGURE 1: (a) Primary structure of the peptide CP-1(CCHH) where positions 3 and 10 are the substitution sites. The internal standard peptide CP-1(CCHC) contains a similar primary sequence with Lys in position 3, Ser in position 10, and Cys in position 24. (b) Structural representation of the metal-bound peptide CP-1(CCHH) displaying the positions of the substitution sites across the β -sheet.

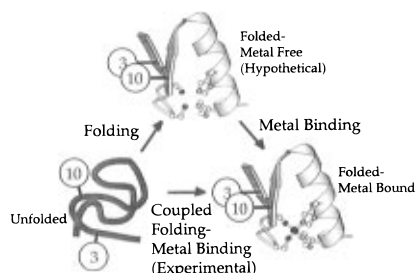


FIGURE 2: Diagram illustrating the relationships between the metal binding, peptide folding, and experimentally derived free energy values.

internal standard (the sequence shown in Figure 1a) were added to the buffer to yield a total peptide concentration of approximately 200 μ M. After addition of both peptides, the pH of the solution dropped to 6.8 and remained constant throughout the experiment. The peptide samples were titrated with Co(II) until both peptides were saturated. The extent of peptide saturation was monitored by the absorbance of the d-d transitions with increasing Co(II). The spectrophotometric assay relies on the deconvolution of different Co(II)-substituted visible spectra of CP-1(CCHH) from the internal standard CP-1(CCHC) as illustrated in Figure 3. The relative fractional saturation of the test peptide relative to the internal standard is used to determine the relative free energy for the coupled metal binding/peptide folding reaction. Spectroscopic measurements were performed on a Perkin-

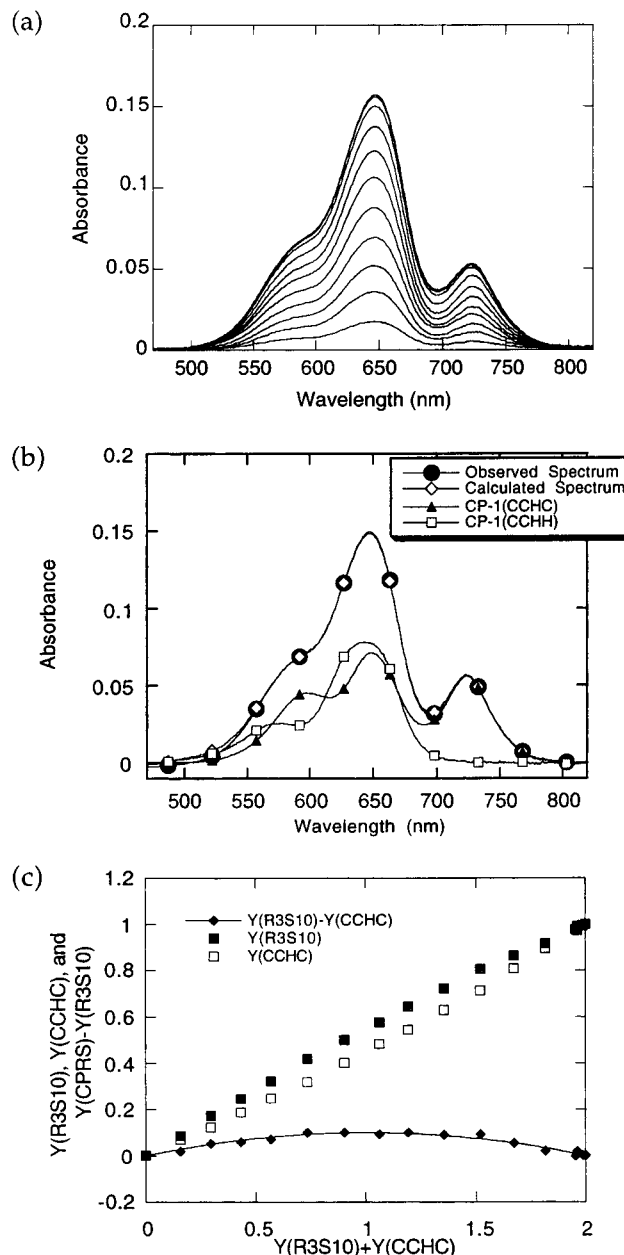


FIGURE 3: (a) Absorption spectra from a cobalt(II) titration involving equimolar amounts of CP-1(CCHH) with Arg in position 3 and Ser in position 10 (R3S10) and CP-1(CCHC). (b) Deconvolution of the one spectrum from the titration into components due to CP-1(CCHH) and CP-1(CCHC). (c) Plot of the fractional saturations of CP-1(CCHH) (R3S10) and CP-1(CCHC) from the titration. The fitted curve is the difference in fractional saturations versus the sum of the fractional saturations of the individual peptides.

Elmer Lambda 9 spectrophotometer at room temperature (23 $^{\circ}$ C).

The resultant absorbance spectra were deconvoluted to yield the coefficients for the individual component absorbance spectra of CP-1(CCHH) and CP-1(CCHC). The fractional saturation of each peptide, Y_1 or Y_2 , was obtained by dividing these coefficients by the total concentration of the individual peptides. These values correspond to the fraction of peptide of each type that has bound cobalt. The data plotted in the form of the difference in fractional saturation versus the sum of the fractional saturation yield a curve that can be fit to yield the value of C , the ratio of the dissociation constants for the two peptides, via the expression (Krizek *et al.*, 1993):

¹ Abbreviations: HEPES, 4-(2-hydroxyethyl)-1-piperazineethanesulfonic acid; the standard one-letter abbreviations are used for the amino acids; CP-1(CCHH) is used to denote the peptide with the sequence ProTyrXaa₃CysProGluCysGlyLysXaa₁₀PheSerGlnLysSerAspLeuVal LysHisGlnArgThrHisThrGly; CP-1(CCHC) is used to denote the peptide ProTyrLysCysProGluCysGlyLysSerPheSerGlnLysSerAspLeuValLysHisGlnArgThrCysThrGly.

$$Y_1 - Y_2 = \{(1 + C) - [(x - 1)^2(1 - C)^2 + 4C]^{1/2}\} / (1 - C) \quad (1)$$

where $x = Y_1 + Y_2$ and $C = K_{d1}/K_{d2} = [Y_2(1 - Y_1)]/[Y_1(1 - Y_2)]$.

A typical curve is shown in Figure 3. Relative free energies were calculated from

$$\Delta\Delta G = -RT \ln (K_{d1}/K_{d2}) / (K_{dS3S10}/K_{d2}) \quad (2)$$

where K_{dS3S10} is the dissociation constant for the CP-1(CCHH) peptide containing Ser residues in both positions 3 and 10, K_{d1} is the dissociation constant for the CP-1(CCHH) peptide under study, and K_{d2} is the dissociation constant for the internal standard CP-1(CCHC) peptide. $\Delta\Delta G$ values were calculated in units of kilocalories per mole at the given salt concentration followed by the standard deviation. At least five titrations were performed at 0.05 M NaCl; three or more titrations were performed for each peptide at other NaCl concentrations. For peptides K3S10 and R3S10, data at 50 mM NaCl were combined with those of Kim and Berg (1993).

Thermodynamic cycles were constructed to relate the S3S10 reference peptide to the doubly mutated peptide with the potential electrostatically interacting residues. The free energy of interaction for each pair was calculated from the difference between the sum of the free energy changes observed for the singly mutated peptide and that observed for the doubly mutated peptide.

RESULTS

Peptides were synthesized with selected amino acids in positions 3 and 10 to test the energetic consequences of various electrostatically related pairs. These sites are shown relative to each other in the tertiary structure of CP-1(CCHH) in Figure 1. Specific combinations of residues at positions 3 and 10 were designed to complete thermodynamic cycles beginning from residue pair S3S10 and ending at the residue pair interaction studied. For instance, to complete the cycle to study the potential salt bridge between K3 and E10, four peptides were investigated: S3S10, K3E10, K3S10, and S3E10. Metal titrations were performed for each of these four peptides using the same internal standard, CP-1(CCHC). The relative free energies of folding were determined from

$$\Delta\Delta G = -RT \ln (K_1/K_2) \quad (3)$$

where K_1 is the relative equilibrium constant derived for the variant peptide and K_2 is the relative equilibrium constant for the S3S10 peptide complex, used as a common reference peptide. The free energy determinations were performed at three NaCl concentrations: 0 mM, 50 mM, and 100 mM. In all cases, the samples included 100 mM HEPES buffer. The $\Delta\Delta G$ values for the relative free energy of folding are presented in Table 1. Thermodynamic cycles and deduced interaction free energies are shown in Figure 4.

DISCUSSION

In keeping with results observed for other systems, the observed free energy changes were relatively modest. Under our standard conditions of 100 mM HEPES, 50 mM NaCl free energy changes (relative to the S3S10 peptide) ranged

Table 1: $\Delta\Delta G$ Values (in kcal/mol) for CP-1(CCHH) with Various Residue Pairs in Positions 3 and 10^a

peptide	0 mM	50 mM	100 mM
S3S10	0	0	0
K3S10	-0.01 ± 0.01	-0.03 ± 0.01	0.06 ± 0.01
R3S10	-0.03 ± 0.01	-0.05 ± 0.01	-0.09 ± 0.01
S3E10	0.06 ± 0.01	-0.04 ± 0.01	-0.08 ± 0.01
K3E10	0.03 ± 0.01	-0.12 ± 0.01	-0.18 ± 0.01
R3E10	-0.05 ± 0.01	-0.11 ± 0.01	-0.13 ± 0.01
S3D10	0.41 ± 0.02	0.19 ± 0.01	0.13 ± 0.01
K3D10	-0.08 ± 0.01	-0.04 ± 0.01	0.07 ± 0.01
R3D10	0.12 ± 0.01	0.03 ± 0.01	0.06 ± 0.01
R3R10	0.26 ± 0.05	0.01 ± 0.01	0.03 ± 0.01
E3E10	0.27 ± 0.03	0.08 ± 0.01	0.01 ± 0.01
K3K10	0.47 ± 0.02	0.22 ± 0.03	0.20 ± 0.02
D3D10	1.36 ± 0.53	1.06 ± 0.43	0.95 ± 0.23

^a The concentration of NaCl utilized is given at the top of each column. Estimated standard errors are also given; the larger error for the value for the D3D10 peptide is due to the larger difference in $\Delta\Delta G$ associated with a given difference in fractional saturation when the cobalt affinities of the peptide being examined and the internal standard peptide differ substantially.

from -0.23 kcal/mol to 0.22 kcal/mol except for the like-charged peptide D3D10 which was destabilized by 1.06 kcal/mol.

In order to determine the electrostatic interaction component for these free energy changes, two additional analyses were performed. First, the free energy determinations were repeated at three NaCl concentrations. Second, interaction free energies were determined through the use of double mutant cycles. In all cases, the relative free energies were nearly constant or become closer to zero as the salt concentration was increased from 0 to 100 mM. The salt dependence is most useful when coupled to the double mutant cycles since this allows isolation of the apparent electrostatic component of the free energy changes.

Thermodynamic cycles for the potential salt bridge pairs are presented in Figure 4a with the concentration of NaCl and the interaction energy noted in the center of each cycle. Double mutant cycles were especially important for peptides with D in position 10 since this sequence change alone introduces a relatively large destabilization of 0.41 kcal/mol in 0 mM NaCl. This destabilization appears to have a substantial electrostatic component since the destabilization decreased significantly as the NaCl concentration was increased. Figure 5 illustrates more clearly the dependence of the interaction energies on the NaCl concentration. The interaction energies for the peptide variants K3D10, R3E10, and R3D10 showed monotonically decreasing stabilizing values with increasing salt concentration. The largest favorable interaction energy of -0.48 kcal/mol was observed for the K3D10 peptide in 0 mM NaCl. The peptide variant K3E10 did not display behavior typical for salt screening of electrostatic effects for unknown reasons. The interaction energies for this ion pair appeared to become more favorable as the NaCl concentration increased although the range was only 0.14 kcal/mol.

To probe the effects of repulsive electrostatic interactions on peptide stability, four peptides containing the like-charged pairs E3E10, D3D10, R3R10, and K3K10 were studied. The four peptides containing these ion pairs are significantly less stable than the reference peptide S3S10 with differences ranging from 0.22 kcal/mol for R3R10 to 1.36 kcal/mol for D3D10. The stability losses decreased with increasing salt

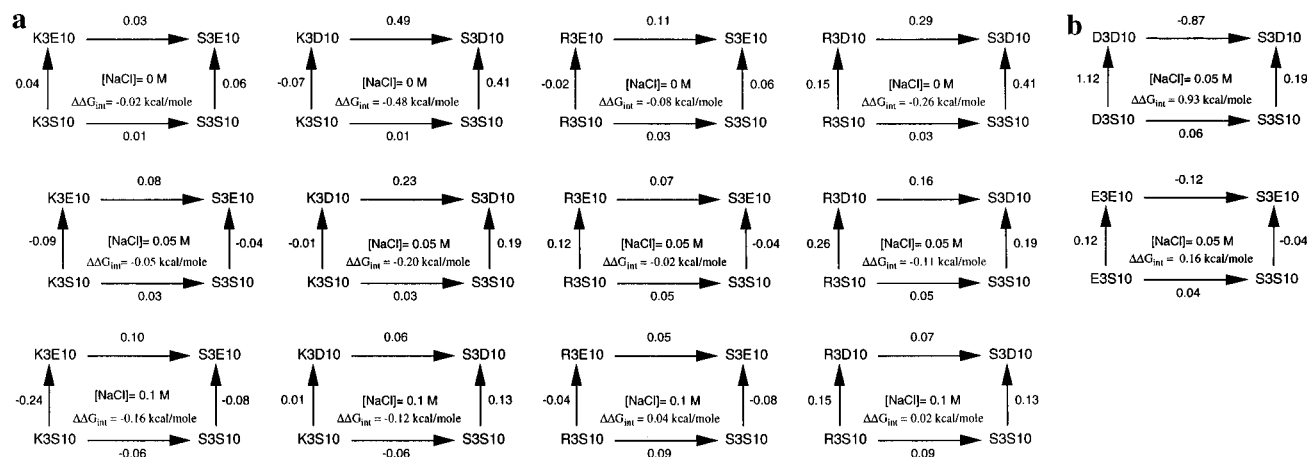


FIGURE 4: (a) Double mutant cycles at various NaCl concentrations. The reference peptide S3S10 is in the lower right corner of each cycle. Values along arrows are in units of kcal/mol; negative signs indicate an increase in stability in the direction of the arrow. Cycles display peptides with oppositely charged residues in positions 3 and 10. The standard deviations are estimated to be ± 0.01 kcal/mol for each $\Delta\Delta G_{int}$ value. (b) Cycles displaying peptides with similarly charged residues in positions 3 and 10. The estimated standard deviations for the $\Delta\Delta G_{int}$ values are ± 0.15 kcal/mol and ± 0.01 kcal/mol for the D3D10 and E3E10 peptides, respectively.

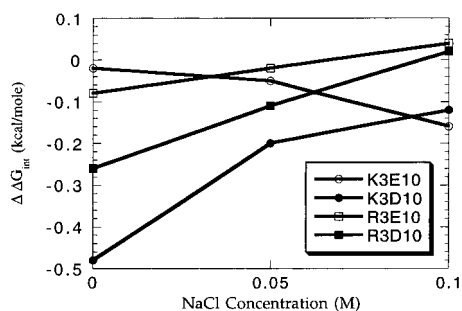


FIGURE 5: Dependence of the interaction free energies for the potential salt bridge-forming peptides on NaCl concentration.

concentration. Further investigations of the repulsive ion pairs of D3D10 and E3E10 were conducted to explore the interaction energies between the residues via double mutant cycles. The thermodynamic cycles for the E3E10 and D3D10 variants are shown in Figure 4b at 50 mM NaCl concentration. The D3D10 pair showed an interaction energy of 0.93 kcal/mol, larger in absolute value than any of the attractive pairs.

The salt bridge free energy values that we report, 0.00–0.48 kcal/mol, are in agreement with other measurements reported for solvent-exposed salt bridges. Lumb and Kim (1995), investigating the electrostatic contributions to the interhelical salt bridges of the GCN4 leucine zipper, concluded that these salt bridges could only maximally contribute 0.5 kcal/mol to protein stability. Other interhelical salt bridges in the triple helix of collagen also contribute an average of 0.5 kcal/mol per individual salt bridge (Vengopul *et al.*, 1994). Even in other proteins, the salt bridge contribution is small. In T4 lysozyme, engineered salt bridges contributed approximately 0.1–0.2 kcal/mol each where most of the increase in energy may be attributable to the interaction of the E or D residue with the helix dipole (Sun *et al.*, 1991a). The protein barnase contains a salt bridge triad composed of D, D, and R. In a mutant where A replaces one of the D residues, one D and R salt bridge contributes 0.22 kcal/mol while the other salt bridge contributes 0.48 kcal/mol (Horovitz *et al.*, 1990). In a model α -helical peptide study, Lyu and co-workers (1992) reported an energetic contribution of 0.5 kcal/mol for an E and K salt bridge. Only one other study to date has investigated

residue pairs in a β -sheet. This study conducted by Smith and Regan (1995) reported that peptides with potential salt bridges across a β -sheet involving E and R were -1.20 kcal/mol more stable than the wild-type, whereas that with E and K was -1.09 kcal/mol more stable. These values were not dissected via salt dependence or double mutant cycles.

A striking feature of our observations is that interactions involving aspartic acid (D) had much more substantial effects than those with other residues, both for the attractive and for the repulsive pairs. For potential salt bridges in α -helical peptides, the reverse has generally been observed. Merutka and Stellwagen (1991), using a model α -helical peptide, studied the same four salt bridges as presented in this work. They found that peptides with D were less stable than those with E when involved with the same potential salt bridging partner. Similar results have been seen by other workers (Huyghues-Despointes *et al.*, 1993; Marqusee & Baldwin, 1990).

Our observations can be rationalized by the following considerations. The formation of a true salt bridge involves at least partial desolvation of the charged residues as well as conformational restriction necessary to maintain the geometric relationship between the interacting residues. Alternatively, the charged residues may interact at a distance without the costs of desolvation and substantial conformational restriction. This, however, decreases the magnitude of the electrostatic interaction. These terms appear to be relatively in balance. In general, we believe that the interaction energies that we have observed are due to interactions at a distance with the geometrical relationship established by the β -sheet but without further restriction. This lack of intimate ion pair formation is consistent with crystallographic observations for a series of exposed potential salt bridging residues (Sun *et al.*, 1991b). In our system, this is supported by the similarity in magnitude between the favorable opposite-charge interactions with those for the repulsive like-charge pairs (when direct interaction is unlikely). The larger effects observed for the interactions involving D are due to the short side chain and concomitant lack of conformational flexibility of this residue. Thus, D may interact more closely with K or R without as large a conformational entropy penalty as that associated with E. This effect is more pronounced for the D3D10 like-charge

pair in which the two negative charges cannot move very far apart because of the short side chains. These effects are different than those in the context of α -helices since the α -carbons bearing the interacting residues are 1–2 Å closer together in a β -sheet than they are in an α -helix. The shorter side chain of D is too short to interact as effectively with the associated positive residue than is that of E in the context of an α -helix.

REFERENCES

- Frankel, A. D., Berg, J. M., & Pabo, C. O. (1987) *Proc. Natl. Acad. Sci. U.S.A.* **84**, 4841–4845.
- Horovitz, A., Serrano, L., Avron, B., Bycroft, M., & Fersht, A. R. (1990) *J. Mol. Biol.* **216**, 1031–1044.
- Huyghues-Despointes, B. M., Scholtz, J. M., & Baldwin, R. L. (1993) *Protein Sci.* **2**, 80–85.
- Kim, C. A., & Berg, J. M. (1994) *Nature* **362**, 267–270.
- Kim, C. A., & Berg, J. M. (1996) *Nat. Struct. Biol.* **3**, 940–945.
- Krizek, B. A., Amann, B. T., Kilfoil, V. J., Merkle, D. L., & Berg, J. M. (1991) *J. Am. Chem. Soc.* **113**, 4518–4523.
- Krizek, B. A., Merkle, D. L., & Berg, J. M. (1993) *Inorg. Chem.* **32**, 937–940.
- Lumb, K. J., & Kim, P. S. (1995) *Science* **268**, 436–439.
- Lyu, P. C., Gans, P. J., & Kallenbach, N. R. (1992) *J. Mol. Biol.* **223**, 343–350.
- Marqusee, S., & Baldwin, R. L. (1987) *Proc. Natl. Acad. Sci. U.S.A.* **84**, 8898–8902.
- Marqusee, S., & Baldwin, R. L. (1990) in *Protein Folding* (Gierasch, L. M., & King, J., Eds.) pp 85–94, American Association for the Advancement of Science, Washington, DC.
- Merutka, G., & Stellwagen, E. (1991) *Biochemistry* **30**, 1591–1594.
- Párraga, G., Horvath, S. J., Eisen, A., Taylor, W. E., Hood, L., Young, E. T., & Klevit, R. E. (1988) *Science* **241**, 1489–1492.
- Smith, C. K., & Regan, L. (1995) *Science* **270**, 980–982.
- Sun, D.-P., Sauer, U., Nicholson, H., & Matthews, B. W. (1991a) *Biochemistry* **30**, 7142–7153.
- Sun, D.-P., Nicholson, H., Baase, W. A., Zhang, X. J., Wozniak, J. A., & Matthews, B. W. (1991b) *Ciba Found. Symp.* **161**, 52–62.
- Venugopal, M. G., Ramshaw, J. A., Braswell, E., Zhu, D., & Brodsky, B. (1994) *Biochemistry* **33**, 7948–7956.
- Vinson, V. K., Amann, B. T., & Berg, J. M. (1996) *Proteins: Struct., Funct., Genet.* (submitted for publication).

BI962805I